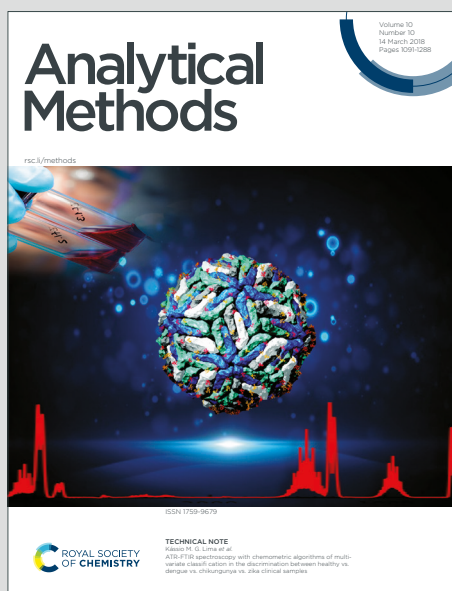


Analytical Methods

Accepted Manuscript

This article can be cited before page numbers have been issued, to do this please use: C. Celik Yoldas, N. Ildiz, P. Sagirolu, M. A. Atalay, N. Y. Demir, M. Duman, B. Cetin, E. Yildirim, G. Can Sezgin, Y. K. Genc, E. Yoldas and I. Ocsoy, *Anal. Methods*, 2026, DOI: 10.1039/D6AY00313C.



This is an Accepted Manuscript, which has been through the Royal Society of Chemistry peer review process and has been accepted for publication.

Accepted Manuscripts are published online shortly after acceptance, before technical editing, formatting and proof reading. Using this free service, authors can make their results available to the community, in citable form, before we publish the edited article. We will replace this Accepted Manuscript with the edited and formatted Advance Article as soon as it is available.

You can find more information about Accepted Manuscripts in the [Information for Authors](#).

Please note that technical editing may introduce minor changes to the text and/or graphics, which may alter content. The journal's standard [Terms & Conditions](#) and the [Ethical guidelines](#) still apply. In no event shall the Royal Society of Chemistry be held responsible for any errors or omissions in this Accepted Manuscript or any consequences arising from the use of any information it contains.

Fast Antibiotic Susceptibility Test Integrated Microfluidic Chips for Detection of Carbapenem/Colistin-Resistant Bacteria by a Smartphone- based Analysis

*Cagla Celik Yoldas, Nilay Ildiz, Pinar Sagiroglu, Mustafa Altay Atalay, Naim Yagiz Demir, Memed Duman, Barbaros Cetin, Ender Yildirim, Gulden Can Sezgin, Yusuf Kenan Genc, Erhan Yoldas, Ismail Ocsoy**

C. Celik Yoldas

Department of Analytical Chemistry, Faculty of Pharmacy, Harran University, 63050, Sanliurfa, Türkiye

N. Ildiz

Medical Imaging Department, Vocational School of Health Services, Bandirma Onyedi Eylul University, 10200, Balikesir, Türkiye

P. Sagiroglu, M. A. Atalay

Department of Medical Microbiology, School of Medicine, Erciyes University, 38039, Kayseri, Türkiye

N. Y. Demir

Department of Oceanography, Institute of Marine Sciences, Middle East Technical University, 33731, Mersin, Türkiye

N. Y. Demir, M. Duman

Nanotechnology and Nanomedicine Division, Institute of Science, Hacettepe University, 06100, Ankara, Türkiye

B. Cetin

Microfluidics & Lab-on-a-chip Research Group, Department of Mech. Eng., İ.D. Bilkent University, 06800, Ankara, Türkiye
UNAM-National Nanotech. Research Center & Inst. Materials Science & Nanotech. İ.D. Bilkent University, 06800, Ankara, Türkiye

E. Yildirim

Department of Mechanical Engineering, Faculty of Engineering, Middle East Technical University, 06800, Cankaya, Ankara, Türkiye
ODTU MEMS Center, 06530, Cankaya, Ankara, Türkiye

G. C. Sezgin

Department of Gastroenterology, Faculty of Medicine, Erciyes University, Kayseri 38039, Türkiye

1
2
3
4
5
6
7
8
9
10
11
12
13
14
15
16
17
18
19
20
21
22
23
24
25
26
27
28
29
30
31
32
33
34
35
36
37
38
39
40
41
42
43
44
45
46
47
48
49
50
51
52
53
54
55
56
57
58
59
60

Y. K. Genc

Hacı Şükrü Baktır Anadolu İmam Hatip High School, 38039, Kayseri, Türkiye
Department of Analytical Chemistry, Faculty of Pharmacy, Erciyes University, 38039, Kayseri,
Türkiye

E. Yoldas

Department of Electrical and Electronics, Faculty of Engineering, Harran University, Sanliurfa
63300, Türkiye

C. Celik Yoldas, I. Ocsoy*

Department of Analytical Chemistry, Faculty of Pharmacy, Erciyes University, 38039, Kayseri,
Türkiye

E-mail: ismailocsoy@erciyes.edu.tr

Phone number: +90 555 088 65 66

Abstract: Although many phenotypic methods have been developed for the detection of antibiotic-resistant bacteria, this emerging field still requires more rapid, practical, and economic approaches. Herein, we report a colorimetric phenotypic antimicrobial susceptibility test integrated into a microfluidic chip (mc-AST) for the detection of carbapenem (Car) and colistin (Col) resistant bacteria. A key component of the mc-AST is anthocyanin, a natural pH indicator that changes color based on the pH of the reaction environment. The mc-AST contains corresponding antibiotics to suppress the growth of susceptible bacteria. The color changes in the mc-AST can be detected by the naked eye and through image processing using a smartphone. The novelty of this study lies in the first-ever integration of an anthocyanin-based antibiotic susceptibility test into a microfluidic chip. This integration provides a resistance profile for multiple doses of antibiotics on a single chip. Ultimately, the mc-AST reduces the workload and delivers results within 2 hours.

Keywords: Antibiotic Susceptibility Test; Colorimetric Assay, Natural pH Indicator; Microfluidic Chips; Carbapenem/Colistin-Resistant Bacteria; Smartphone-based Analysis

Introduction

Antimicrobial resistance (AMR) can be considered as a silent epidemic that has been growing stronger for years. The current methods have not been fully effective in prevention and management of AMR. World Health Organization (WHO) and the United Nations (UN) have taken serious responsibilities in preparation global action plan to combat resistant microorganisms. ¹ The UN General Assembly mentioned the critical importance of AMR with High-Level Meeting in 2016. The countries have been encouraged to develop national action plans to reduce AMR and to secure people against threats of bacterial AMR in the future.² Despite preventive measures and innovative decisions, the number of deaths associated with bacterial AMR is estimated to be 4.95 million in 2019. Unfortunately, the worldwide death count due to AMR is estimated to reach 10 million by 2050. The health economic impact of this disease is estimated to be \$100 trillion at US.¹ The top six pathogens responsible for resistance-related deaths are *Acinetobacter baumannii*, *Klebsiella pneumoniae*, *Escherichia coli*, *Staphylococcus aureus*, *Streptococcus pneumoniae* and *Pseudomonas aeruginosa*.³ Carbapenem resistance has been reported at the critical level in the list of "Bacterial Priority Pathogens" announced by the WHO Core Package of Interventions to Support National Action Plans. The WHO updated the Bacterial Priority Pathogens List (BPPL) in 2024, which includes 15 families of antibiotic-resistant bacteria grouped into critical, high and medium categories for prioritization. Carbapenem-resistant *Acinetobacter baumannii* is ranked first in the BPPL. ^{4, 5} The announced plan reported that AMR could be prevented with four basic components, one of which is early, rapid and accurate diagnosis. The 33 research priorities for bacterial and fungal infections are grouped into four themes. Investigation and evaluation of rapid point-of-care (POC) diagnostic tests ranks 6th behind prevention parameters. ⁵ This was highlighted as a priority that because more effective methods are highly needed for pathogen detection, rapid identification of antibiotic resistance and implementation of urgent and accurate treatment. Rapid diagnostic tests and/or methods are still required to help healthcare professionals make the right choice of antibiotics. These tests will shorten the treatment process and limit the use of antibiotics. Except malaria and HIV, only 19% of people in low- and middle-income countries have access to simple diagnostic tests to guide antibiotic prescribing in primary care.^{5,6}

The current gold standard for antimicrobial susceptibility testing (AST) is culture-based methods such as agar diffusion, disc diffusion and broth dilution. These methods rely on the bacterial growth. However, they present several drawbacks including 18-24 hours (hrs) incubation time, intensive labor work and multiple steps ⁷. Apart from phenotypic methods, genotypic methods

1
2
3
4
5
6
7
8
9
10
11
12
13
14
15
16
17
18
19
20
21
22
23
24
25
26
27
28
29
30
31
32
33
34
35
36
37
38
39
40
41
42
43
44
45
46
47
48
49
50
51
52
53
54
55
56
57
58
59
60
106

CC BY-NC
This article is licensed under a Creative Commons Attribution-NonCommercial 3.0 Unported Licence.
DOI: 10.1039/D6AY00313C
View Article Online
DOI: 10.1039/D6AY00313C

are also available like polymerase chain reaction (PCR), which aims to detect resistance genes, gives rapid results, spectroscopic methods for monitoring bacterial growth and mass spectrometric methods for biochemical analysis. However, they have several disadvantages, such as the need of expensive equipment, specialized staff and high cost.^{8,10} In view of these problems, there is a high demand for rapid, cost-effective, user-friendly and accurate POC tests. Microfluidics has become popular as a promising diagnostic technique for AST development. The importance of POC diagnostics was highlighted during the pandemic. In the fight against antibiotics, it will be the most important tool with high specificity analysis. Features such as rapid results, high efficiency, minimal sample requirements and cost effectiveness are the main reasons for choosing microfluidics based POC diagnostics.^{7,11} The results of color-based microfluidic sensors are based on the detection and evaluation of individual colors. Mathematical models can be used to accurately determine colors. The CIELab formula, one of the models developed for this purpose, divides each color into three components. Lightness (0-100) is the space between black and white, a is the space between green and red (-128, +127) and b is the space between blue and yellow (-128, +127). All colors that the human eye can see and distinguish can be represented in this space. Based on this formula, the formula ΔE_{ab} is used to calculate the difference between two colors. This formula is also used in the analysis of test results.¹²

$$\Delta E_{ab}^* = \sqrt{(L_2^* - L_1^*)^2 + (a_2^* - a_1^*)^2 + (b_2^* - b_1^*)^2}$$

Color space values categorized as RGB (red, green, blue), HSV, HSL, CMYK and CIE give results proportional to the concentration of analyte. However, color image processing techniques can be performed in computer-based software. In this case, the end user must be a professional. In recent years, smartphones have become an indispensable tool for POC testing. This is due to their popularity, portability and improvements in software.^{13,14} Smartphone-based POC assays are preferred because of their widespread availability, accessibility, usability, low cost and rapid analysis.¹⁵ In many tests that make direct measurements from different samples such as urine and plasma, the analysis is based on color image processing using smartphones. To protect the analysis results from external factors, standardization is ensured by the development of a photo box and phone apparatus.^{11,16-18} Here, we have developed a colorimetric microfluidic chip-integrated AST (mc-AST) that gives results in 2 hrs. The mc-AST was designed for detection of carbapenem (Car) and colistin (Col) (last resort but have high resistance rates) antibiotic resistant bacteria. The colorimetric mc-AST solution contains anthocyanin groups, which are pH indicators extracted from plants,

1
2
3
4
5
6
7
8
9
10
11
12
13
14
15
16
17
18
19
20
21
22
23
24
25
26
27
28
29
30
31
32
33
34
35
36
37
38
39
40
41
42
43
44
45
46
47
48
49
50
51
52
53
54
55
56
57
58
59
60

CC BY-NC

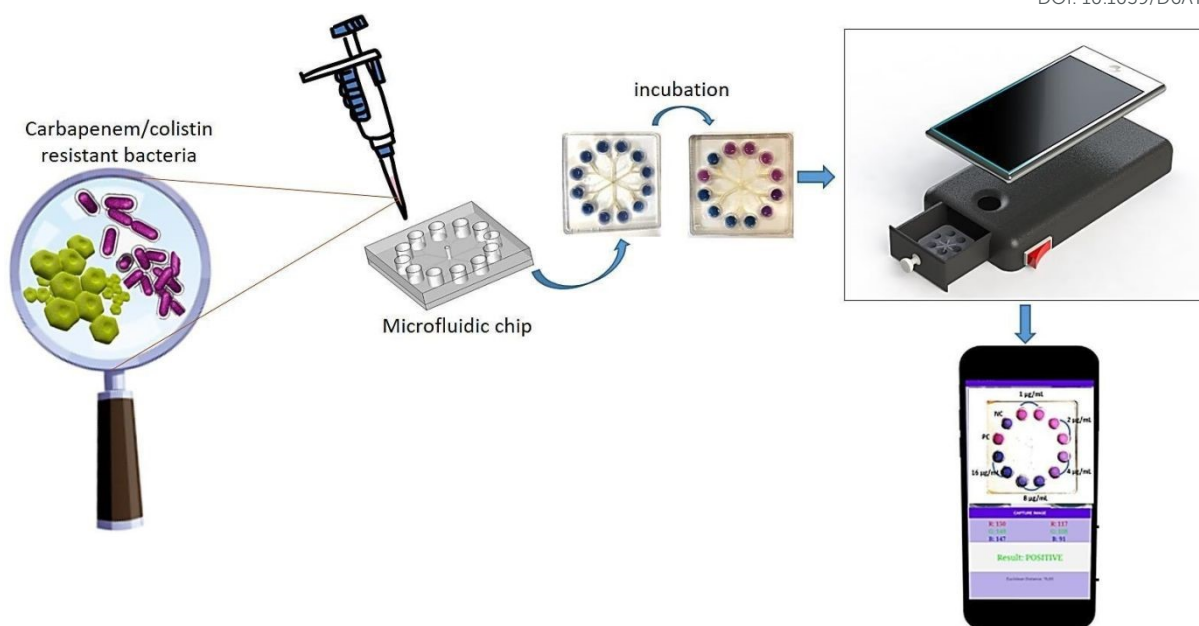
1
2
3
4
5
6
7
8
9
10
11
12
13
14
15
16
17
18
19
20
21
22
23
24
25
26
27
28
29
30
31
32
33
34
35
36
37
38
39
40
41
42
43
44
45
46
47
48
49
50
51
52
53
54
55
56
57
58
59
60

culture media and appropriate antibiotics. The current test solution is deposited into the microfluidic chip, revealing the resistance profile to multiple doses of antibiotics on a single chip. As the bacteria continue their vital activities in the chip-well, acidic volatile gases (AVG) are released. The susceptible bacteria do not release AVG owing to inhibition of their growth and then the pH remains constant and therefore, no color change is observed. In contrast to that, when bacterial strains are resistant towards antibiotics, color and pH values of mc-AST are changed due to production of AVG. We developed a mobile application that performs color image processing to increase the sensitivity of mc-AST results based on color change. We also developed a mobile phone apparatus to standardize the results. Microfluidic chips reduce the workload of AST, which requires a time-consuming process, and reveals the resistance profile to several different doses at the same time. Thus, a fast, sensitive and innovative mc-AST was developed.

Results and Discussion

In this study, we prepared natural pH indicator based colorimetric test solutions integrated to microfluidic chips fabricated with various designs for detection of carbapenem and colistin resistant bacteria. The colorimetric responses were witnessed by a naked eye and smartphone readouts containing Red-Green-Blue (RGB) and Delta-E (ΔE) analysis. The anthocyanin molecules used as a key component in colorimetric test change reaction color in the presence of antibiotic resistance bacteria. As bacteria grow, their metabolism produces AVG. The organic acids produced in this process cause the pH of the medium to decrease. In the test medium, anthocyanins act as pH indicators, so they protonate as the medium becomes acidic, changing color from blue (basic) to pink. Bacterial metabolism is inhibited by carbapenem/colistin, preventing acid production. The stable structure of the anthocyanin molecules is retained and their initial blue color is maintained due to the absence of AVG in the medium. The test response time relies on bacteria concentration and microfluidic chips designs. The **Scheme 1** clearly show preparation of colorimetric microfluidic chip based test and detection of corresponding bacteria by a naked eye and digital image analysis based upon color change.

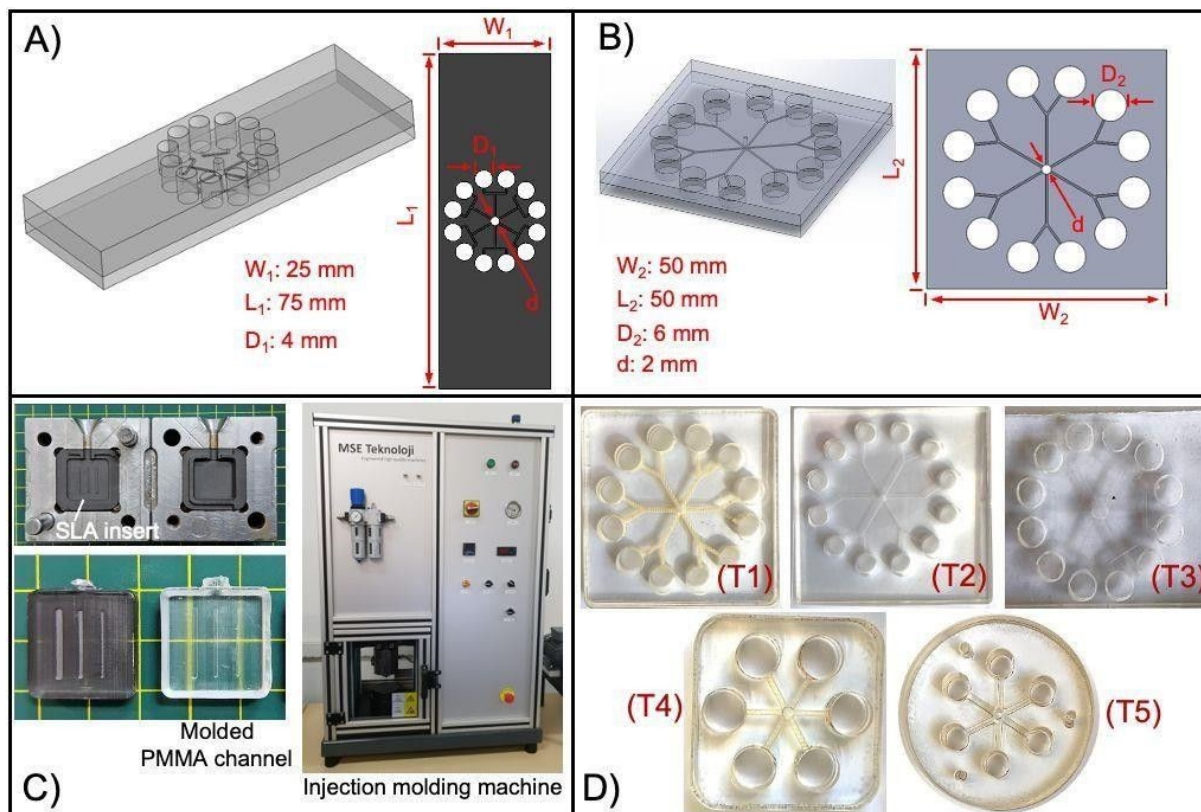
Scheme 1.

View Article Online
DOI: 10.1039/D6AY00313C

Schematic illustration of colorimetric test integrated microfluidic chips for detection of carbapenem and colistin resistant bacteria by a naked eye and smartphone analysis.

It is worthy to mention that integration of colorimetric test solutions to various microfluidic chips. These microfluidic chips were fabricated with different designs and stages.

Fig. 1

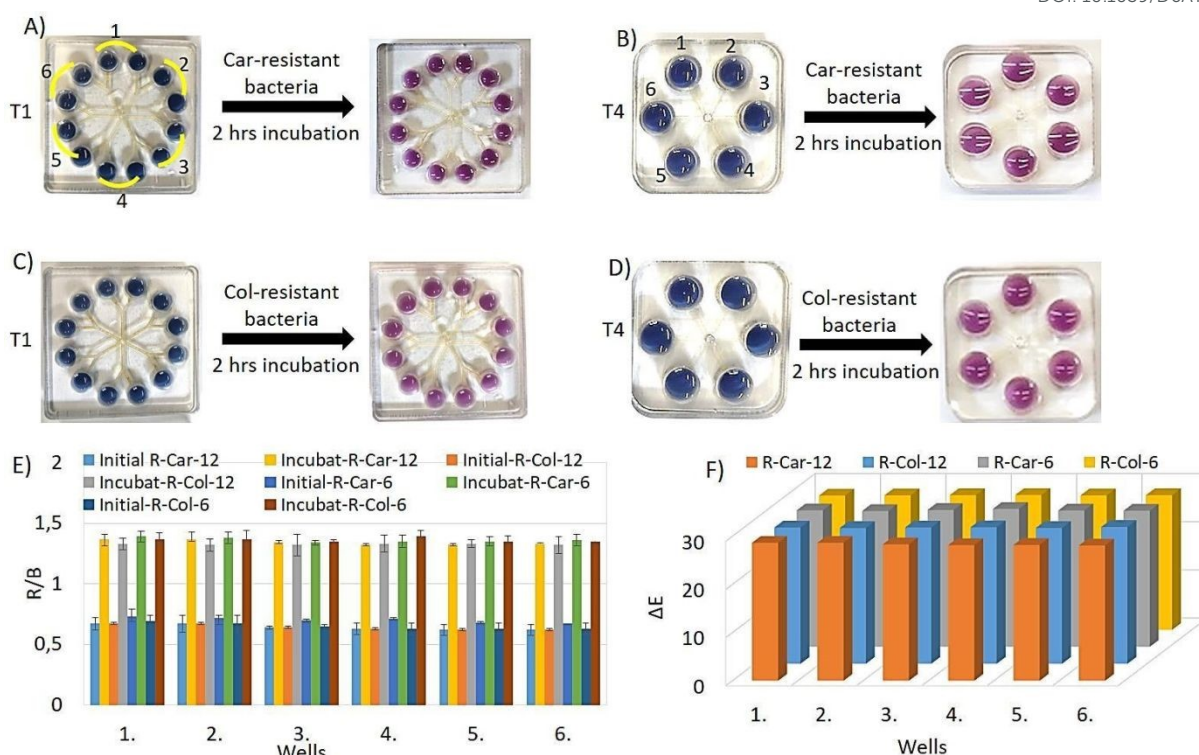


1
2
3
4
5
6
7
8
9
10
11
12
13
14
15
16
17
18
19
20
21
22
23
24
25
26
27
28
29
30
31
32
33
34
35
36
37
38
39
40
41
42
43
44
45
46
47
48
49
50
51
52
53
54
55
56
57
58
59
60

Microfluidic chip designs and stages A) First generation design B) Second generation design C) Production stages to be used in mass production. Appearance of microfluidic chips prepared with different designs D) 12-well microfluidic chips (T1, T2, T3) and 6-well microfluidic chips (T4, T5).

In the first step, all wells of the chips were spiked with 8 ppm carbapenem to detect antibiotic resistant bacteria. This was a proof-of-concept for simultaneous color change, as this high concentration would be expected to inhibit susceptible strains while resistant strains continue to live. We prepared test solution composed of 25% RCE extract as a source of anthocyanin acting pH indicator and carbapenem resistant bacterial strain suspension at pH 8 with blue color. The 1200 μ L and 600 μ L of test solution was deposited into T1 type 12-well and T4 type 6-well microfluidic chips respectively. After 2 hours (hrs) incubation, blue color of the test solution in all 12-well and 6-well microfluidic chips was converted into pinkish color as shown in Figure 2A and 2B, respectively. The content and volume of colorimetric test solution in 12-well and 6-well microfluidic chips remained the same, except replacing antibiotic type from carbapenem to colistin, for analysis of colistin resistant bacteria. The goal of this experiment is to prove that the color change is simultaneous in wells loaded with the same dose of antibiotic. This was done by controlling the flow of liquid through the channels in the designed microfluidic chips. The microfluidic chips were left for 2 hrs incubation, then distinct occurrence of pink color was observed in both 12-well and 6-well microfluidic chips as presented in Figure 2C and 2D. We believe that the color changes in the each well rely on protonation of anthocyanin molecules. Although colorimetric tests include antibiotics, resistant bacteria continuously grow and make reaction environment acidic owing to their AVOCs production. The hydroxyl groups of anthocyanin molecules were protonated at acidic pH and their electron density was changed, both of which induce color change from blue to pink. While colorimetric responses were seen by a naked eye, the color changes in the each well was analyzed by smartphone based ImageJ software including Red/Blue (R/B) and Delta-E (ΔE) calculation. As an example, the clear differences in R/B and ΔE values before and after addition of antibiotics resistant bacteria were produced in Figure 2E and 2F, respectively, which can be considered as a semi-quantitative and supportive results for colorimetric detection.

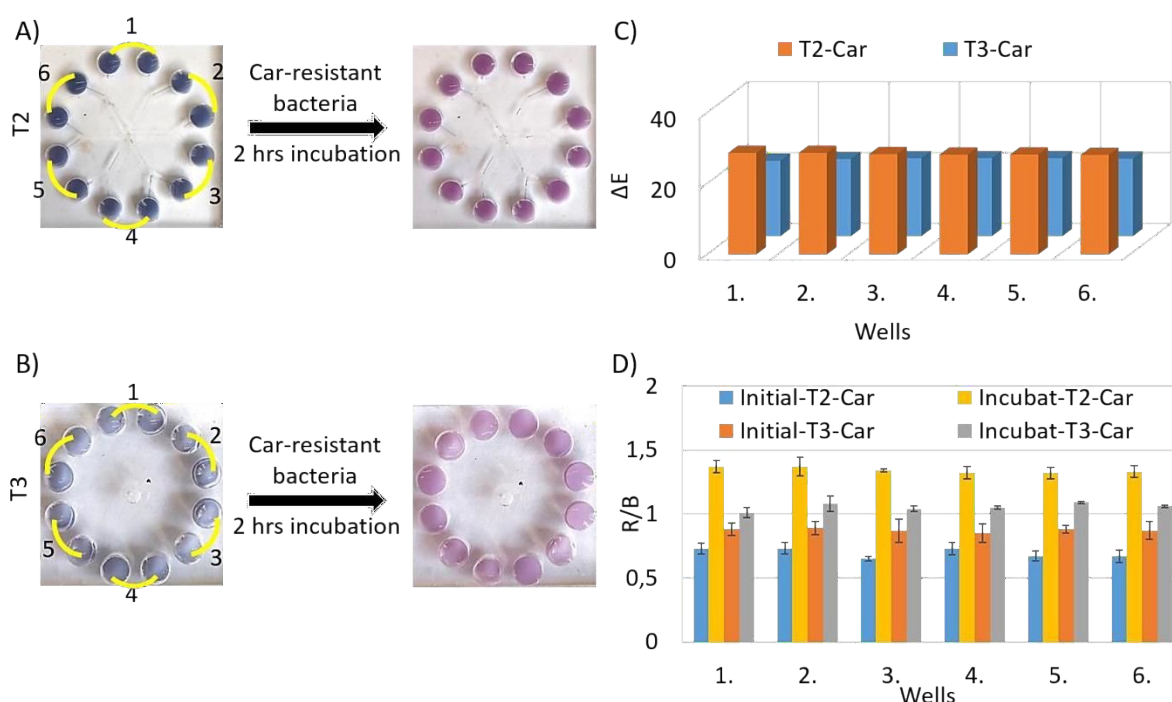
Fig. 2

View Article Online
DOI: 10.1039/D6AY00313C

Color change observed in the presence of resistant bacteria in T1 type 12-well microfluidic chips and T4 type 6-well microfluidic chips. A) Carbapenem resistance analysis in T1 type microfluidic chips B) Carbapenem resistance analysis in T4 type microfluidic chips C) Colistin resistance analysis in T1 type microfluidic chips D) Colistin resistance analysis in T4 type microfluidic chips. Antibiotic: 2 ppm, Bacteria: 3 McFarland. E) RGB analysis. F) Delta E analysis.

In order to show how type of microfluidic chips affect response time of the test solution, we combined the same test solution contained carbapenem resistant bacterial strain with T2 type and T3 type 12-well microfluidic chips. We demonstrated that dark and light blue color of initial test solutions were turned to dark and light pink colors in 2 hrs incubation in T2 type (Figure 3A) and T3 type (Figure 3B) microfluidic chips. These visual colorimetric readouts were analyzed with ΔE and R/B calculations presented in Figure 3C and 3D, respectively. The remarkable and acceptable differences in ΔE and R/B values were calculated in 2 hrs incubation.

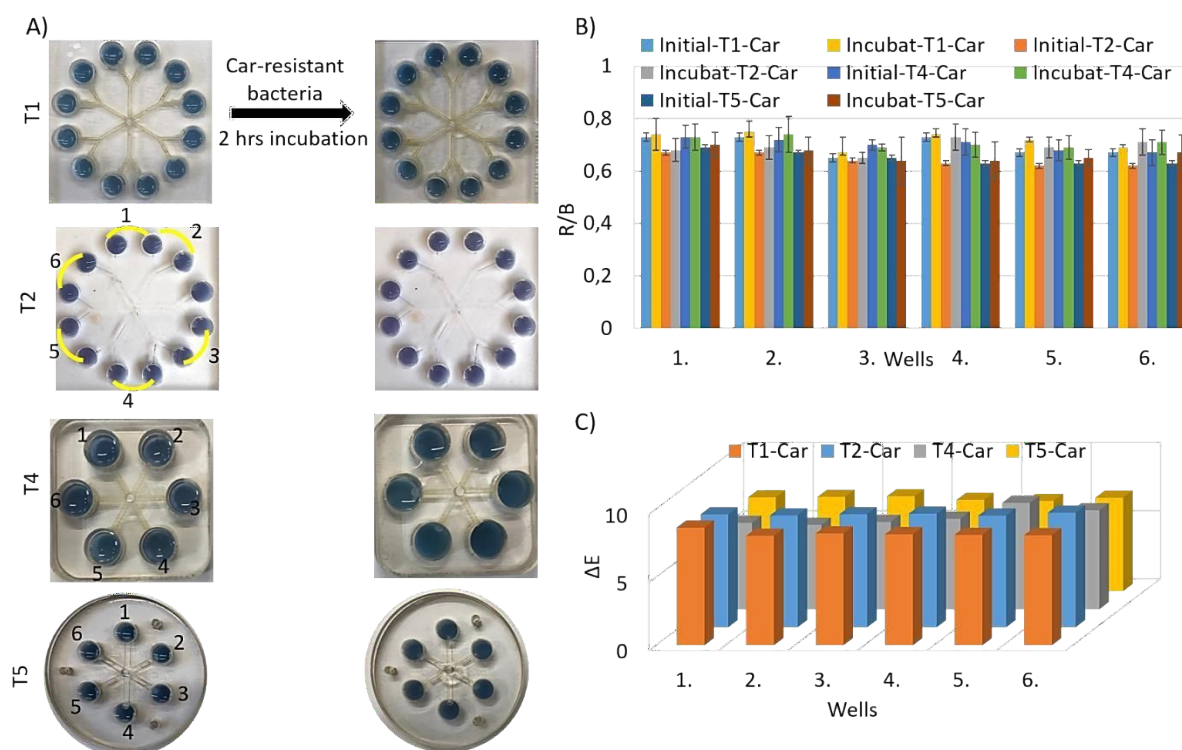
Fig. 3

View Article Online
DOI: 10.1039/D6AY00313C

Color change observed in the presence of Carbapenem-resistant bacteria in 12-well microfluidic chips A) Carbapenem-resistant bacteria in Type 2 microfluidic chips B) Carbapenem-resistant bacteria in Type 3 microfluidic chips C) RGB analysis D) Delta E analysis.

As a further systematic study, we investigated stability and specificity of colorimetric test solution integrated into four types of microfluidic chips including T1 type 12-well (Figure 4A), T2 type 12-well (Figure 4B), T4 type 6-well (Figure 4C), and T5 type 6-well (Figure 4D) microfluidic chips towards carbapenem susceptible strain. After 2 hrs incubations, no color change was observed by a naked eye in all microfluidic chips. We interpret that growth of susceptible strain was inhibited due the presence of 8 ppm carbapenem in test solution, then pH values of reaction solution remained the same. As long as pH of reaction solution is not changed, the pH indicator does not loss or gain proton, then color of initial test solutions are not changed. In addition to that, the test solution was quite stable because its initial color was constant before and after addition susceptible bacterial strain.

Fig. 4

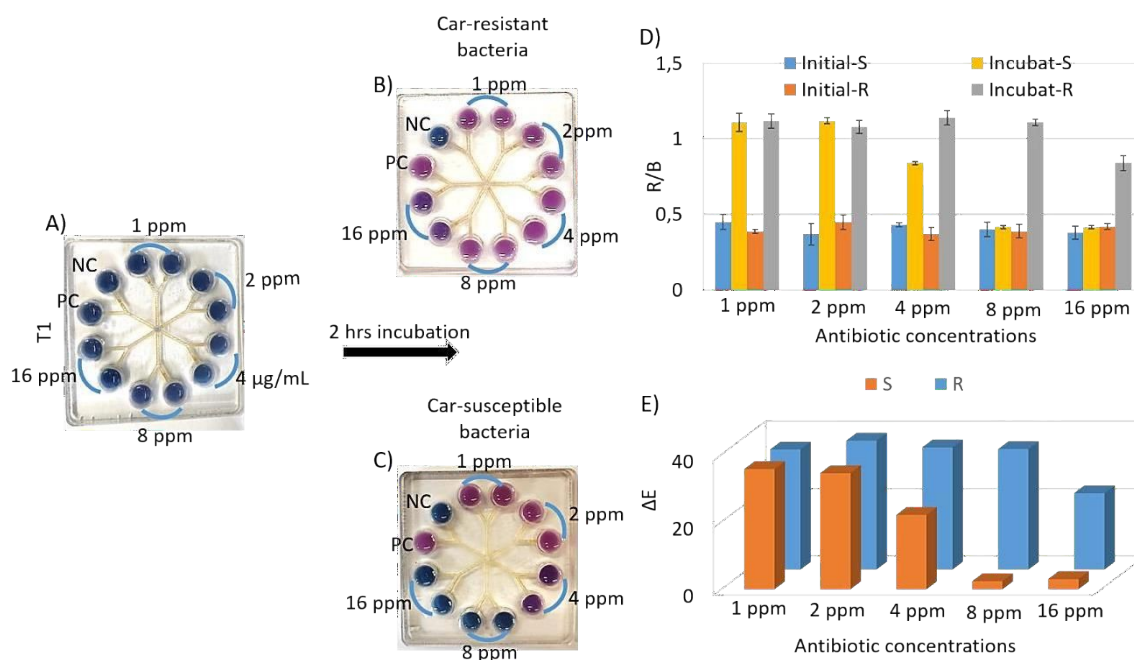


Colorimetric results observed in 12-well microfluidic chips (T1 and T2) and 6-well microfluidic chips (T4 and T5) in the presence of carbapenem susceptible strain. Antibiotic: 32 ppm, Bacteria: 3 McFarland. A) Carbapenem- susceptible bacteria in Type 1, Type 2, Type 4, and Type 5 microfluidic chips B) RGB analysis C) Delta E analysis.

We manipulated concentration of antibiotics in test solution in order to determine how antibiotic affect detection of target bacteria. We prepared blue color test solutions with a series concentration of carbapenem (1 ppm, 2 ppm, 4 ppm, 8 ppm and 16 ppm) in each well of T1 type of microfluidic chips for detection of carbapenem susceptible strain bacteria (Figure 5A). For instance, while initial blue color test solutions with 1 ppm, 2 ppm, 4 ppm and 8 ppm were turned clear pink color in the presence of Carbapenem-resistant bacteria within 2 hrs incubation, however, 16 ppm carbapenem included test solution was turned into purple color (Figure 5B). We propose that Carbapenem resistant bacteria actively grown in 8 ppm carbapenem included test solution, but they partially or slowly grown in test solution with 16 ppm carbapenem. The test solution called “Negative Control (NC) containing 32 ppm carbapenem completely inhibited growth of the resistant bacteria, then blue color of the test solution was not changed. The Positive Control (PC) test solution does not contain antibiotic, then its blue color was converted into pink color due to bacterial growth. In the presence of carbapenem susceptible strain, blue color of test solutions with 1 ppm and 2 ppm was turned to pink color (Figure 5B).

We claim that antibiotic used with 1 ppm and 2 ppm was not able to suppress the growth of these susceptible bacteria. Additionally, 4 ppm carbapenem used in test solution partially inhibited bacterial growth since not clear color change was observed. The test solutions including 8 ppm, 16 ppm and 32 ppm (Negative Control) carbapenem completely stopped growth of susceptible bacteria. The blue color of test solution without antibiotic rapidly turned to pink color in the growth of susceptible bacteria. All colorimetric responses in the presence of resistant and susceptible bacteria in microfluidic chips observed by a naked eye were well-consistent with R/B and ΔE analysis, respectively presented in Figure 5D and 5E.

Fig. 5

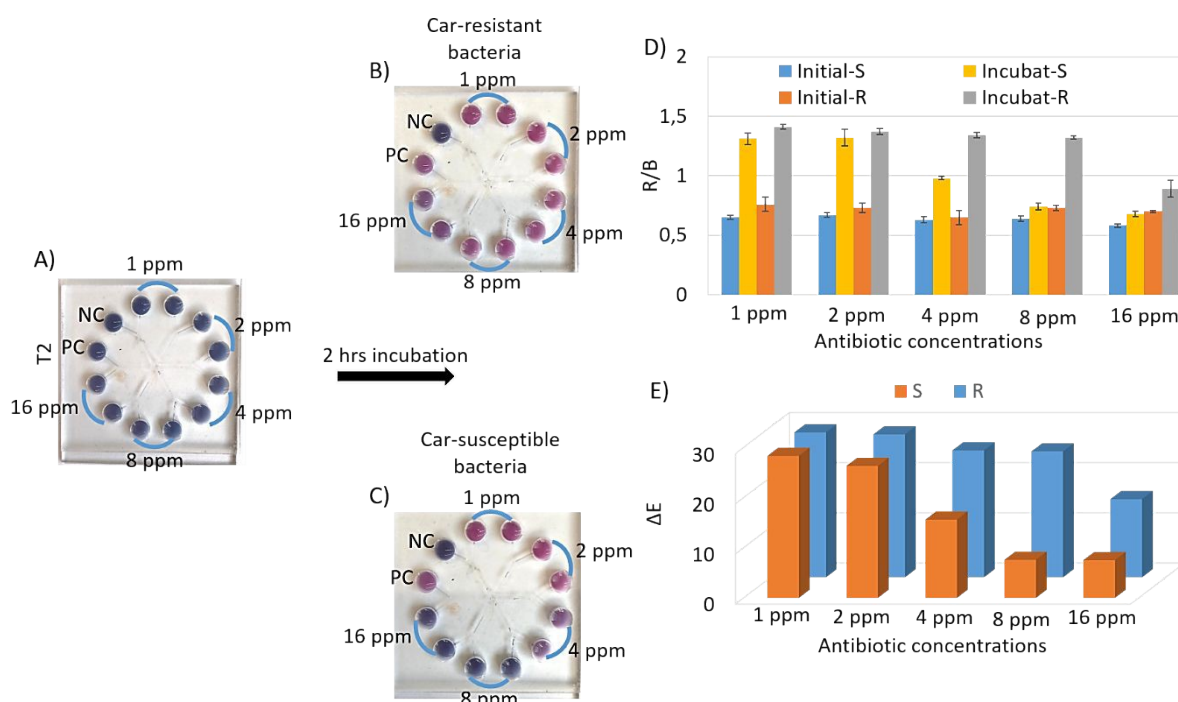


Analysis of carbapenem-resistant and susceptible strains in the anthocyanin-based phenotypic carbapenem susceptibility test integrated into T1 type 12 well microfluidic chips. A) Appearance of the test with carbapenem-resistant strain added before incubation B) Color change of the test with carbapenem-resistant strain added at the end of incubation period C) Color change of the test with carbapenem-susceptible strain added at the end of incubation period D) RGB analysis E) Delta E analysis. NC: 32 ppm. Bacteria: 3 McFarland.

In order to elucidate effect of microfluidic chips type, we adapted all experiments made in Figure 5 to Figure 6 by just only T1 type 12-well microfluidic chips with T2 type for detection of carbapenem resistant bacteria. We revealed that initial blue color test solutions with 1 ppm, 2 ppm, 4 ppm, 8 ppm and 16 ppm carbapenem concentrations in T2 type 12-well microfluidic chips (Figure 6A) were clearly turned to pink color in the presence of Carbapenem-resistant bacteria within 2 hrs incubation (Figure 6B). The behavior of negative Control (including 32 ppm and positive Control (no antibiotic included) gave the same response with

Figure 5B. The carbapenem susceptible strains were added into each well of T2 type microfluidic chips, while no bacterial growth was observed in 8 ppm and above carbapenem concentrations, but these bacteria continued to grow in test solution including under 8 ppm carbapenem concentrations (Figure 6C). The smartphone based digital imaging processing system produced the same results for R/B and ΔE analysis in Figure 6D and 6E, respectively as given in Figure 5D and 5E.

Fig. 6



Analysis of carbapenem-resistant and susceptible strains in the anthocyanin-based phenotypic carbapenem susceptibility test integrated into T2 type 12 well microfluidic chips. A) Appearance of the test with carbapenem-resistant strain added before incubation B) Color change of the test with carbapenem-resistant strain added at the end of incubation period C) Color change of the test with carbapenem-susceptible strain added at the end of incubation period D) RGB analysis E) Delta E analysis. NC: 32 ppm. Bacteria: 3 McFarland.

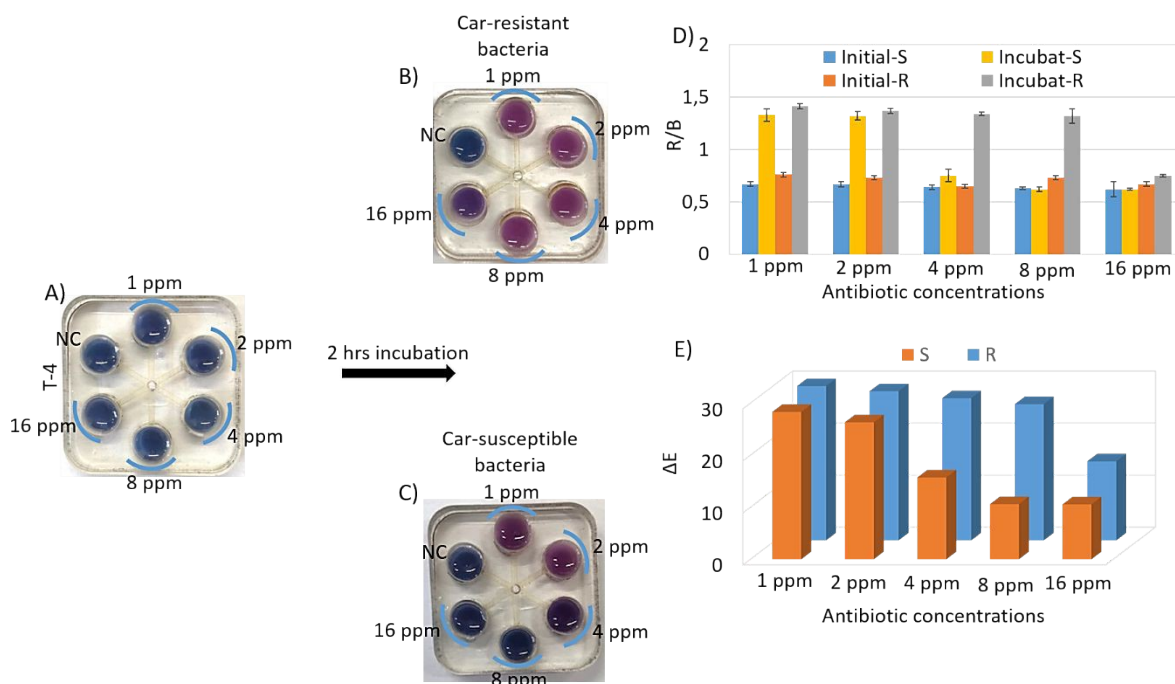
We further examine how 6-well microfluidic chips called “T4 type” influence detection of carbapenem resistant compared to other microfluidic chips. We demonstrated that initial blue color test solutions with 1 ppm, 2 ppm, 4 ppm and 8 ppm carbapenem was changed to pink color in the presence of carbapenem-resistant bacteria (Figure 7A and 7B). When carbapenem concentration increased to 16 ppm, blue color of the test solution was turned to purple color in the 2 hrs incubation due partial growth of carbapenem-resistant bacteria. The Negative Control test solution (including 32 ppm carbapenem) completely inhibited growth of the bacteria, then initial blue color remained consistent. While carbapenem susceptible strains changed the color

of the test solutions including 1 ppm and 2 ppm carbapenem from blue to pink (Figure 7C). While the test solution with 4 ppm carbapenem was converted from blue to purple, but no susceptible bacterial growth was observed in 8 ppm and above carbapenem concentrations. The R/B and ΔE calculations in Figure 7D and 7E, respectively were well consistent with colorimetric responses visualized by a naked eye.

We systematically investigate stability of the test colorimetric test solutions in detection of carbapenem-resistant strains (Figure 8A). We prepared test solutions with blue color at pH 8 and stored them at +4 °C and -20 °C for 1 month, 3 months and 6 months. We added carbapenem-susceptible bacterial suspensions into well no 1 and no 4 including 8 ppm carbapenem, of 1 month, 3 months and 6 months stored test solution stored at +4 °C and -20 °C, initial blue color of the test solutions was not changed. We conclude that both the test solutions were quite stable and no susceptible bacteria were grown. However, the same test solutions under the same experimental parameters were used for detection of carbapenem-resistant bacteria. The regardless of any storage time of the test solutions, the carbapenem-resistant bacteria deposited into well no 2 and no 5 changed blue color to pink at +4 °C and -20 °C with 2 hrs incubation. We claim that the test solutions stored at any temperatures and till 6 months can be used as freshly prepared for detection of antibiotic-resistant bacteria. In terms of the smartphone based digital image processing, the colorimetric responses were supported by R/B and by ΔE analysis, respectively presented in Figure 8B and 8C. The distinct differences in R/B ratio and ΔE value allow us to distinguish antibiotic resistant bacteria compared to susceptible ones.

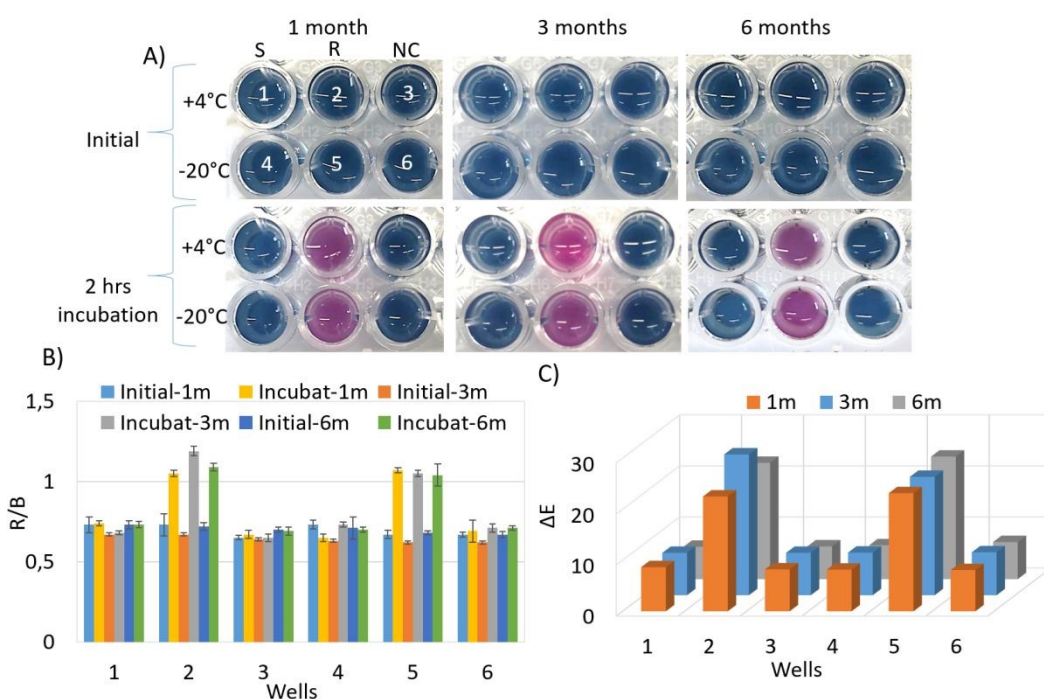
Fig. 7

View Article Online
DOI: 10.1039/D6AY00313C



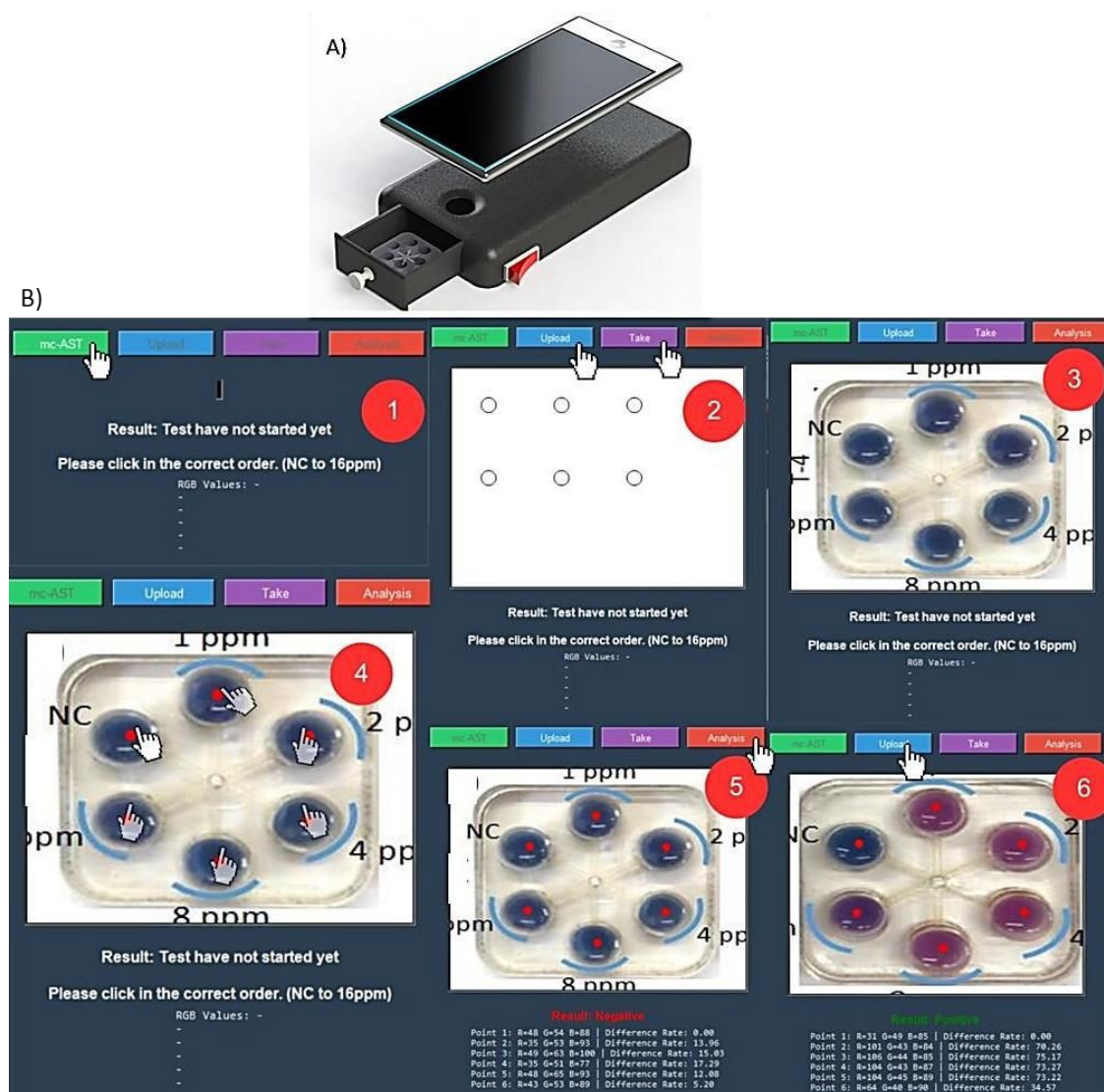
Analysis of carbapenem-resistant and susceptible strains in the anthocyanin-based phenotypic carbapenem susceptibility test integrated into T4 type 6 well microfluidic chips. A) Appearance of the test with carbapenem-resistant strain added before incubation B) Color change of the test with carbapenem-resistant strain added at the end of incubation period C) Color change of the test with carbapenem-susceptible strain added at the end of incubation period D) RGB analysis E) Delta E analysis. NC: 32 ppm. Bacteria: 3 McFarland.

Fig. 8



Color changes observed in the presence of resistant and sensitive bacteria in test solutions incubated at +4 °C and -20 °C for 1, 3 and 6 months. A) Colorimetric results B) RGB analysis C) Delta E analysis.

Fig. 9



Smartphone platform and mobile application interfaces A) Components of the smartphone platform B) Interfaces of smartphone applications.

3D-printed smartphone platform was developed and used to analyze digital images with R/B and ΔE calculations as illustrated in Figure 9. Figure 9A shows that the components of the smartphone platform composed of the camera, LED, and sample holder coupled with computer assisted design (CAD) software. In terms of working mechanism, the initial blue of test solutions (pH 8) were converted to pink color in the presence of colistin or carbapenem resistant clinical bacterial strains. The interfaces of the smartphone application are shown in Figure 9B. The mobile application provides the test results through a user friendly interface.



Compared to our earlier manual assays, the microfluidic platform has simplified the analytical workflow by replacing repetitive dilutions with a single-step procedure for loading the sample using ready-to-use reagents. Relying on the device's internal fluidic layout rather than manual volume adjustments significantly minimises user-induced errors during sample distribution. Furthermore, reducing the necessary equipment to just one chip and pipette tip removes labour-intensive steps, demonstrating the platform's potential for high-throughput applications.

Conclusion

In summary, we have developed microfluidic chip-integrated a colorimetric phenotypic antimicrobial susceptibility tests (mc-AST) for detection of carbapenem (Car) and colistin (Col) antibiotic resistant bacteria. Our study demonstrated that mc-AST was efficiently used for reducing detection time and revealing the resistance profile to several different doses at the same time. The antibiotic resistant bacteria released AVG during their growth and made reaction environment acidic, in which anthocyanin molecule called “pH indicator” was protonated and change the color change in the chip-well, respectively. The color changes were observed by a naked eye and digital imaging processing (ΔE and R/B analysis). The mc-AST showed great stability in time interval of 1, 3 and 6 months.

Materials and Methods

Materials and Instruments: Tryptic soy agar (Merck, Germany), agar (Merck, Germany), skimmed milk medium (Difco, USA), meat extract (Acumedia, UK), NaCl (Isolab, Türkiye), peptone (Mast Diagnostic, UK), carbapenem (Merck, Germany) and colistin (Merck, Germany) were all purchased from the companies indicated.

Microorganisms: Resistant and susceptible bacterial pathogens: *Acinetobacter baumannii* ATCC BAA-1710, *Acinetobacter baumannii* ATCC BAA-1792, *Klebsiella pneumoniae* ATCC 13883, *Klebsiella pneumoniae* ATCC BAA-3067 and *Escherichia coli* ATCC 25922 were obtained from Erciyes University, Faculty of Pharmacy, Pharmaceutical Microbiology research laboratory ATCC culture collection. All pathogens were stored in skim milk medium at $-20\text{ }^{\circ}\text{C}$ and regenerated prior to the experiments. The optical density was determined by spectrophotometer (Azure Ao, Azure Biosystems, Inc.).

Red Cabbage (*Brassica oleracea*) Extraction: Red cabbage (*Brassica oleracea* L.; family *Brassicaceae*) is used to extract anthocyanin, one of the main components in antibiotic susceptibility testing. In the first stage of extraction, the leaves of this plant, which is rich in

1
2
3 cyanidin-3-diglucoside-5-glucoside, are separated, cleaned, and cut into small pieces. One
4 hundred grams of the plant material was boiled in 100 grams of distilled water for 30 minutes
5 in a 1:1 wt/wt ratio. Finally, the extract is filtered with Whatman No. 1 filter paper. The obtained
6 extract is purple and has a pH value of 7.0. The extract was stored in amber-colored glass bottles
7 at 4 °C for use in the test content.¹⁹
8
9
10

View Article Online
DOI: 10.1039/D6AY00313C

Analytical Methods Accepted Manuscript

11
12
13
14
15
16
17
18
19
20
21
22
23
24
25
26
27
28
29
30
31
32
33
34
35
36
37
38
39
40
41
42
43
44
45
46
47
48
49
50
51
52
53
54
55
56
57
58
59
60



Design of Microfluidic Chips: Microfluidic chips were designed within the Microfluidics and Lab-on-a-Chip Research Group at Bilkent University. The first-generation design comprised a single inlet (d: 2 mm) and twelve outlet wells (D1: 4 mm), interconnected via microchannels with a width of 0.4 mm and a height of 0.2 mm (Figure 2A). The first-generation prototype was manufactured using micromilling at the Micro Manufacturing Laboratory at Middle East Technical University. The chip was fabricated on a 3 mm thick polymethyl methacrylate (PMMA) substrate with standard microscope slide dimensions of 25 × 75 mm, using a CNC milling machine (PROXXON FF500/BL CNC Milling Machine, PROXXON GmbH, Hetzerath, Germany). The microchannels were machined using a 0.4 mm diameter end mill, with a spindle speed of 4000 rpm, a feed rate of 30 mm/min, and a depth of cut of 0.1 mm. The terminal cavities of the channels were created using a 2 mm diameter end mill at the same spindle speed, with an increased feed rate of 50 mm/min. During the experiments, it was observed that sharp corners at the bifurcation points of the microchannel create cleaning difficulties. In the second-generation design, these corners were rounded to facilitate more effective maintenance and reduce the risk of contamination. The second-generation design retained the overall architectural layout (Figure 2B); however, the outlet wells were redesigned with a reduced diameter of 3.3 mm. Consequently, the volume of each outlet well increased from 38 μL to 200 μL. The manufacturing of the second-generation design was also performed via milling (PROXXON FF500/BL-CNC) on two PMMA plates, each with a thickness of 3 mm, forming a structure with overall dimensions of 50 mm × 50 mm. The microchannels were machined using a 0.4 mm diameter tool at a spindle speed of 4000 rpm and a feed rate of 30 mm/min. A 6 mm diameter tool was used to drill the holes and cavities. On one of the plates, microchannels with a width of 0.4 mm and a depth of 0.2 mm were patterned, along with 6 mm diameter through-holes located at the ends of the channels. The second PMMA plate featured 6 mm diameter, 2 mm deep cavities positioned to align with the holes on the first plate. The patterned PMMA plates were then exposed to chloroform vapor for 3 minutes to locally soften the surfaces, enabling temporary adhesion. Subsequently, the plates were thermally bonded under a hot press by applying a force of 1000 N at 72°C for 30 minutes.

Although the method used is suitable for prototyping, the chip must be compatible with injection molding for high-volume manufacturing.²⁰ Considering the channel dimensions in the second-generation design, it was assessed that the design could also be fabricated using injection molding to support scalability. To evaluate this, injection molding trials were

1
2
3
4
5
6
7
8
9
10
11
12
13
14
15
16
17
18
19
20
21
22
23
24
25
26
27
28
29
30
31
32
33
34
35
36
37
38
39
40
41
42
43
44
45
46
47
48
49
50
51
52
53
54
55
56
57
58
59
60

1
2
3
4
5
6
7
8
9
10
11
12
13
14
15
16
17
18
19
20
21
22
23
24
25
26
27
28
29
30
31
32
33
34
35
36
37
38
39
40
41
42
43
44
45
46
47
48
49
50
51
52
53
54
55
56
57
58
59
60
61
62
63
64
65
66
67
68
69
70
71
72
73
74
75
76
77
78
79
80
81
82
83
84
85
86
87
88
89
90
91
92
93
94
95
96
97
98
99
100
101
102
103
104
105
106
107
108
109
110
111
112
113
114
115
116
117
118
119
120
121
122
123
124
125
126
127
128
129
130
131
132
133
134
135
136
137
138
139
140
141
142
143
144
145
146
147
148
149
150
151
152
153
154
155
156
157
158
159
160
161
162
163
164
165
166
167
168
169
170
171
172
173
174
175
176
177
178
179
180
181
182
183
184
185
186
187
188
189
190
191
192
193
194
195
196
197
198
199
200
201
202
203
204
205
206
207
208
209
210
211
212
213
214
215
216
217
218
219
220
221
222
223
224
225
226
227
228
229
230
231
232
233
234
235
236
237
238
239
240
241
242
243
244
245
246
247
248
249
250
251
252
253
254
255
256
257
258
259
260
261
262
263
264
265
266
267
268
269
270
271
272
273
274
275
276
277
278
279
280
281
282
283
284
285
286
287
288
289
290
291
292
293
294
295
296
297
298
299
300
301
302
303
304
305
306
307
308
309
310
311
312
313
314
315
316
317
318
319
320
321
322
323
324
325
326
327
328
329
330
331
332
333
334
335
336
337
338
339
340
341
342
343
344
345
346
347
348
349
350
351
352
353
354
355
356
357
358
359
360
361
362
363
364
365
366
367
368
369
370
371
372
373
374
375
376
377
378
379
380
381
382
383
384
385
386
387
388
389
390
391
392
393
394
395
396
397
398
399
400
401
402
403
404
405
406
407
408
409
410
411
412
413
414
415
416
417
418
419
420
421
422
423
424
425
426
427
428
429
430
431
432
433
434
435
436
437
438
439
440
441
442
443
444
445
446
447
448
449
450
451
452
453
454
455
456
457
458
459
460
461
462
463
464
465
466
467
468
469
470
471
472
473
474
475
476
477
478
479
480
481
482
483
484
485
486
487
488
489
490
491
492
493
494
495
496
497
498
499
500
501
502
503
504
505
506
507
508
509
510
511
512
513
514
515
516
517
518
519
520
521
522
523
524
525
526
527
528
529
530
531
532
533
534
535
536
537
538
539
540
541
542
543
544
545
546
547
548
549
550
551
552
553
554
555
556
557
558
559
560
561
562
563
564
565
566
567
568
569
570
571
572
573
574
575
576
577
578
579
580
581
582
583
584
585
586
587
588
589
590
591
592
593
594
595
596
597
598
599
600
601
602
603
604
605
606
607
608
609
610
611
612
613
614
615
616
617
618
619
620
621
622
623
624
625
626
627
628
629
630
631
632
633
634
635
636
637
638
639
640
641
642
643
644
645
646
647
648
649
650
651
652
653
654
655
656
657
658
659
660
661
662
663
664
665
666
667
668
669
670
671
672
673
674
675
676
677
678
679
680
681
682
683
684
685
686
687
688
689
690
691
692
693
694
695
696
697
698
699
700
701
702
703
704
705
706
707
708
709
710
711
712
713
714
715
716
717
718
719
720
721
722
723
724
725
726
727
728
729
730
731
732
733
734
735
736
737
738
739
740
741
742
743
744
745
746
747
748
749
750
751
752
753
754
755
756
757
758
759
760
761
762
763
764
765
766
767
768
769
770
771
772
773
774
775
776
777
778
779
780
781
782
783
784
785
786
787
788
789
790
791
792
793
794
795
796
797
798
799
800
801
802
803
804
805
806
807
808
809
810
811
812
813
814
815
816
817
818
819
820
821
822
823
824
825
826
827
828
829
830
831
832
833
834
835
836
837
838
839
840
841
842
843
844
845
846
847
848
849
850
851
852
853
854
855
856
857
858
859
860
861
862
863
864
865
866
867
868
869
870
871
872
873
874
875
876
877
878
879
880
881
882
883
884
885
886
887
888
889
890
891
892
893
894
895
896
897
898
899
900
901
902
903
904
905
906
907
908
909
910
911
912
913
914
915
916
917
918
919
920
921
922
923
924
925
926
927
928
929
930
931
932
933
934
935
936
937
938
939
940
941
942
943
944
945
946
947
948
949
950
951
952
953
954
955
956
957
958
959
960
961
962
963
964
965
966
967
968
969
970
971
972
973
974
975
976
977
978
979
980
981
982
983
984
985
986
987
988
989
990
991
992
993
994
995
996
997
998
999
1000

conducted at the Micro Manufacturing Laboratory. During the trials, an insert mold featuring channels with widths of 0.2 mm, 0.5 mm, and 1.0 mm (each with a height of 0.2 mm, resulting in aspect ratios of 1, 0.4, and 0.2, respectively) was produced using a stereolithography (SLA) 3D printer (Form 3, FormLabs, Somerville, MA, USA) (Figure 2C). PMMA pellets were injected into the mold using a plunger-type injection molder (IM_2500_30_300, MSE Technology, Istanbul, Türkiye) at a barrel temperature of 230 °C. The results confirmed that the smallest channels (0.2 mm wide with an aspect ratio of 1.0) could be successfully replicated using this method, demonstrating the moldability of the features on the microfluidic chips.

Preparation of Fast Antibiotic Susceptibility Test-Integrated Microfluidic Chips: Colorimetric assays containing anthocyanins were prepared in solution form with minor modifications of the reported studies.^{21,24} In brief, the first step in preparing the test was sterilizing the basic components — 10 g/L peptone, 1 g/L meat extract, and 75 g/L salt — in an autoclave at 121 °C for 15 minutes. The second step was to adjust the red cabbage extract solution to pH 8.0 with 1 M NaOH solution. After filter sterilization, the solution was added to the test medium at a ratio of 1:1.

Firstly, carbapenem/colistin solution prepared by serial dilution is added to the wells of the microfluidic chips as positive control, negative control, 1-2-4-8-16 ppm doses. Tests for carbapenem/colistin-resistant bacteria have been developed in accordance with the European Committee on Antimicrobial Susceptibility Testing (EUCAST) 2026 guidelines. For susceptible strains of *Acinetobacter baumannii*, *Klebsiella pneumoniae*, and *Escherichia coli*, these concentrations were determined based on the concentration ranges corresponding to the antibiotic MIC cutoff values specified in the EUCAST 2026 guidelines. Bacteria surviving in wells containing antibiotics at these concentrations are considered resistant strains. This design provides a rapid testing platform for detecting carbapenem/colistin-resistant bacteria.²⁵ The antibiotic volumes added in this step were standardized to 5 µL. They were dried at 37°C in a static, closed environment in an incubator without shaking.

The test solution containing anthocyanin and the bacterial suspension to be tested for resistance profile were mixed in a 1:1 ratio. Antibiotic-loaded microfluidic chips were also dried in an incubator and then dispensed through the central inlet hole so that each well contained 100 µL of anthocyanin-containing test medium. 1200 µL (for 12-wells chip) and 600 µL (for 6-wells chip) of test solution were added to the wells. 200 µL and 300 µL of test media were tested and did not provide the desired yield. The microfluidic chips were incubated for four hours at 37 °C in a stationary medium (without shaking) after the inoculation. The channels were filled

with mineral oil and put inside a humidified Petri dish to avoid the test solution from entering them or returning to the central intake hole, as well as minimize evaporation and possible cross-contamination. Throughout the experiment, this setup eliminated desiccation and maintained a consistent reaction volume. The color change in the wells is recorded over time.

Digital Image Processing: For digital image processing, microfluidics are placed on a white background and photographed. The captured images are saved in JPEG format. ImageJ software (National Institutes of Health) was used to analyze color changes in the microfluidic wells. ImageJ software was used to calculate the RGB (red, green, blue) analysis averages and the Euclidean distance (Delta E) in the wells. To quantify color change, all pixels in the images were divided into red, green, and blue components, and the mean values of the R, G, and B channels were calculated. In color image processing, the Delta E formula, derived from the CIE 1976 Lab color difference formula, was applied to compare initial and incubation color changes. The ΔE formula is based on measuring color differences between two images.^{26,27}

$$\Delta E = [(\Delta L)^2 + (\Delta a)^2 + (\Delta b)^2]^{1/2} \quad (1)$$

L^* , a^* , and b^* in the formula represent the dimensions of the CIE Lab color space. The a-axis ranges from red (+a) to green (-a); the b-axis ranges from yellow (+b) to blue (-b); and the L-axis ranges from black (0) to white (100). According to these parameters, the color difference is low in similar images and increases in different images.^{28,29} The ΔE value is a numerical indicator of the limits at which the human eye can distinguish between two colors. Thus, the color difference in the developed colorimetric test provides a more accurate indication of the presence of bacteria.

Development of a Smartphone Application: A custom smartphone application with image processing functionality was developed using Python. The application has the ability to run from Android 4 to Android 10. The mobile application does not require an Ethernet connection to access the camera and files on the device. The main menu consists of a "Please click in the correct order" button to launch the menu. This interface provides instructions for capture the image and analysis steps. After photographing the microfluidic chips, the Red Green Blue (RGB) values of each wells of microfluidic chip image are calculated. These values are used in the Euclidean distance formula. After analysis, all RGB values, the Euclidean distance result, and the final test result are displayed at the bottom of the screen. The Euclidean distance (ED) formula (Equation 2) is shown below.^{30,31}

$$ED^2 = (R_2 - R_1)^2 + (G_2 - G_1)^2 + (B_2 - B_1)^2 \quad (2)$$

1
2
3
4
5
6
7
8
9
10
11
12
13
14
15
16
17
18
19
20
21
22
23
24
25
26
27
28
29
30
31
32
33
34
35
36
37
38
39
40
41
42
43
44
45
46
47
48
49
50
51
52
53
54
55
56
57
58
59
60

CC BY-NC
This article is licensed under a Creative Commons Attribution-NonCommercial 3.0 Unported Licence.

(2) For values of 25 and above, the screen displays positive, confirming the presence of antibiotic resistant bacteria. Based on repeated experiments with susceptible and resistant standard strains, we defined a threshold value for the Euclidean distance. The Euclidean distance (ED) values for the datasets illustrated in Figures 5, 6, and 7 are provided in the supplementary material for reference. To obtain reliable and highly accurate results the camera should be held in the same position as much as possible to avoid focusing on the background or other objects. This is not always possible. Therefore, a smartphone platform has been developed to standardize the distance of the camera from the chips and to achieve an even lighting environment. Thanks to the platform, reliable results can be obtained.

Versatile 3D-Printed Smartphone Platform Design: A smartphone platform was designed for imaging the chips. This design is a more compact version of our previous platform.³² The platform consists of two components: a drawer for holding the chips and a stand for the smartphone. The drawer includes a slot to position the chips and prevent movement. The stand features an opening aligned with the smartphone camera. Inside the stand, a battery and a white LED light are integrated. The system is controlled via an on/off switch. The platform was fabricated using an Ultimaker S3 3D printer with black tough poly(lactic acid) (PLA) at 20% infill. Figure 9A presents an overview of the design, which has been modified in this study to specifically fit the Xiaomi Redmi 10S model by adjusting the slot in the drawer and the camera opening.

Acknowledgments

Funding: This work is financially supported by grants awarded from the The Scientific and Technological Research Council of Türkiye with 122S090 project code.

We would like to thank Yusuf Dogan for his assistance in drawing and designing scheme. This work was supported by the The Scientific and Technological Research Council of Türkiye with 122S090 project code.

Author Contributions

C.C.Y. ran all experiments as the first author. The project was conveyed and designed by I.O. as a correspond author. N.I., P.S., M.A.A., N.Y.D., M.D., B.C., E.Y., G.C.S., Y.K.G., E.Y. contributed to the experiments. N.I., P.S., M.A.A., N.Y.D., M.D., B.C., E.Y., G.C.S., Y.K.G., E.Y. and I.O. supervised all experiments. All authors wrote the manuscript.

References

- 1- Shatalin, K. *et al.* Inhibitors of bacterial H₂S biogenesis targeting antibiotic resistance and tolerance. *Sci.* **372**, 1169-1175 (2021).

- 1
2
3
4
5
6
7
8
9
10
11
12
13
14
15
16
17
18
19
20
21
22
23
24
25
26
27
28
29
30
31
32
33
34
35
36
37
38
39
40
41
42
43
44
45
46
47
48
49
50
51
52
53
54
55
56
57
58
59
60
61
62
63
64
65
66
67
68
69
70
71
72
73
74
75
76
77
78
79
80
81
82
83
84
85
86
87
88
89
90
91
92
93
94
95
96
97
98
99
100
- 2- Walsh, T. R., Gales, A. C., Laxminarayan, R., Dodd, P. C. Antimicrobial resistance: addressing a global threat to humanity. *PLoS Med.* **20**, e1004264 (2023). View Article Online
DOI: 10.1039/D6AY00313C
- 3- Murray, C. J. *et al.* Global burden of bacterial antimicrobial resistance in 2019: a systematic analysis. *The lancet* **399**, 629-655 (2022).
- 4- WHO Updates List of Drug Resistant Bacteria Most Threatening to Human Health. <https://www.who.int/news/item/17-05-2024-who-updates-list-of-drug-resistant-bacteria-most-threatening-to-human-health>, (2024) (accessed: May 2025).
- 5- Minimum requirements for infection prevention and control programmes. Geneva: World Health Organization. <https://apps.who.int/iris/handle/10665/330080>, (2019) (accessed May 2025).
- 6- People-centred approach to addressing antimicrobial resistance in human health: WHO core package of interventions to support national action plans. <https://www.who.int/publications/i/item/9789240082496> (2023) (accessed May 2025).
- 7- Qureshi, Y. Z. A. N., Li, M., Chang, H., Song, Y. Microfluidic chip systems for color-based antimicrobial susceptibility test A review. *Biosens. Bioelectron.* **117160**, (2025).
- 8- Yusoof, K. A. *et al.* Tuberculosis phenotypic and genotypic drug susceptibility testing and immunodiagnosics: a review. *Front. Immunol.* **13**, 1–13 (2022).
- 9- Vasala, A., Hytönen, V. P., Laitinen, O. H. Modern Tools for Rapid Diagnostics of Antimicrobial Resistance. *Front. Cell. Infect. Microbiol.* **10**, (2020).
- 10- Gopalakrishnan, S., Mall, D., Pushpavanam, S., Karmakar, R. Rapid antimicrobial susceptibility testing using carbon screen printed electrodes in a microfluidic device. *Sci. Rep.* **15**, 5133 (2025).
- 11- Pang, Z. *et al.* A self-priming digital microfluidic chip for single-cell antibiotic susceptibility testing. *Microchem. J.* **209**, 112685 (2025).
- 12- Mokrzycki, W. S., Tatol, M. Colour difference ΔE EA survey. *Mach. Graph. Vis.* **20**, 383-411 (2011).
- 13- Xiao, M. *et al.* Virus detection: from state of the art laboratories to smartphone based point of care testing. *Adv. Sci.* **9**, Article, 2105904 (2022).
- 14- Wang, B. *et al.* Smartphone-based platforms implementing microfluidic detection with image-based artificial intelligence. *Nat. Commun.* **14**, 1-18 (2023).
- 15- Chunta, S. *et al.* Point-of-care blood tests using a smartphone-based colorimetric analyzer for health check-up. *Microchim. A.* **191**, 402 (2024).
- 16- Fan, K. *et al.* Digital quantification method for sensitive point-of-care detection of salivary uric acid using smartphone-assisted μ PADs. *ACS Sens.* **7**, 2049-2057 (2022).
- 17- Biswas, S.K. *et al.* Instrument-free single-step direct estimation of the plasma glucose

- level from one drop of blood using smartphone-interfaced analytics on a paper strip.
Lab Chip **22**, 4666-4679 (2022). View Article Online
DOI: 10.1039/D6AY00313C
- 18- Rahman, M.M., Uddin, M.J., Hong, J.H., Bhuiyan, N.H., Shim, J.S., Lab-in-a-Cup (LiC): An au-tonomous fluidic device for daily urinalysis using smartphone Sensor. *Actuat. B-Chem.* **355. Article**, 131336-355 (2022).
- 19- Shalaby, S. M.; Amin, H. H., Red Cabbage and Turmeric Extracts as Potential Natural Colors and Antioxidants Additives in Stirred Yogurt. *J. Probiotics Health* **6**, 206 (2018).
- 20- Çetin, B., Koska, A. K., Erdal, M. Warp-age characterization of microchannels fabricated by injection molding. *J. Micro Nanomanuf.* **3**, 1–7 (2015).
- 21- Celik, C. *et al.* Novel anthocyanin-based colorimetric assay for the rapid, sensitive, and quantitative detection of helicobacter pylori. *Anal. Chem.* **93**, 6246-6253 (2021).
- 22- Celik, C., Ildiz, N., Kaya, M. Z., Kilic, A. B., Ocoy, I. Preparation of natural indicator incorporated media and its logical use as a colorimetric biosensor for rapid and sensitive detection of Methicillin-resistant Staphylococcus aureus. *Anal. Chim. Acta* **1128**, 80-89 (2020).
- 23- Yilmaz, C. *et al.* Recent Trends and Advances in Design of Rapid Tests for Colorimetric Detection of Staphylococcus aureus. *IntechOpen* Ch.3 (2024).
- 24- Celik, C. *et al.* Preparation of nature inspired indicator based agar for detection and identification of MRSA and MRSE. *Talanta* **219**, 121292 (2020).
- 25- The European Committee on Antimicrobial Susceptibility Testing, Breakpoint tables for interpretation of MICs and zone diameters Version 16.0. <https://www.eucast.org/bacteria/clinical-breakpoints-and-interpretation/clinical-breakpoint-tables/>, **2026** (accessed 30 May 2026).
- 26- Soldat, D. J., Barak, P., Lepore, B. J. Microscale colorimetric analysis using a desktop scanner and automated digital image analysis. *J. Chem. Educ.* **86**, 617 (2009).
- 27- Capitán-Vallvey, L. F., López-Ruiz, N., Martínez-Olmos, A., Erenas, M. M., Palma, A. J., Recent developments in computer vision-based analytical chemistry: A tutorial review. *Anal. Chim. Acta* **899**, 23–56 (2015).
- 28- Gao, L., Ren, W., Li, F., Cheng, H. M., Total color difference for rapid and accurate identification of grapheme. *ACS Nano* **2**, 1625–1633 (2008).
- 29- Kılıc, V. *et al.* Single-Image Referenced Colorimetric Water Quality Detection Using a Smartphone. *ACS Omega* **3**, 5531–5536 (2018).
- 30- Tsyrlneva, I., Alagappan, P., Liedberg, B. Colorimetric detection of salivary α -amylase using maltose as a noncompetitive inhibitor for polysaccharide cleavage. *ACS Sens.* **4**, 865–873 (2019).

- 1
2
31- Wesolkowski, S., Color image edge detection and segmentation: a comparison of the
vector angle and the euclidean distance color similarity measures (Master's thesis,
University of Waterloo), (1999). New Article Online
DOI: 10.1039/D6AY00313C
- 32- Celik, C., Demir, N. Y., Duman, M., Ildiz, N., Ocsoy, I., Red cabbage extract-mediated
colorimetric sensor for swift, sensitive and economic detection of urease-positive
bacteria by naked eye and Smartphone platform. *Sci. Rep.* **13**, 2056 (2023).

1
2
3
4
5
6
7
8
9
10
11
12
13
14
15
16
17
18
19
20
21
22
23
24
25
26
27
28
29
30
31
32
33
34
35
36
37
38
39
40
41
42
43
44
45
46
47
48
49
50
51
52
53
54
55
56
57
58
59
60

Open Access Article. Published on 05 June 2026. Downloaded on 06/29/2026 12:09:55 PM.
This article is licensed under a Creative Commons Attribution-NonCommercial 3.0 Unported Licence.



Analytical Methods Accepted Manuscript

Data Availability Statement

[View Article Online](#)
DOI: 10.1039/D6AY00313C

The data supporting this article have been included as part of the Supplementary Information.

1
2
3
4
5
6
7
8
9
10
11
12
13
14
15
16
17
18
19
20
21
22
23
24
25
26
27
28
29
30
31
32
33
34
35
36
37
38
39
40
41
42
43
44
45
46
47
48
49
50
51
52
53
54
55
56
57
58
59
60

Open Access Article. Published on 05 June 2026. Downloaded on 06/29/2026 12:09:55 PM.
This article is licensed under a Creative Commons Attribution-NonCommercial 3.0 Unported Licence.

